UNIVERSITY OF CALIFORNIA
Los Angeles

Phase Behavior of Particle-Polyelectrolyte Complexes

A thesis submitted in partial satisfaction

of the requirements for the degree Master of Science

in Chemical Engineering

by

John E. Neilsen

2019

ABSTRACT OF THE THESIS

Phase Behavior of Particle-Polyelectrolyte Complexes

by

John Neilsen

Master of Science in Chemical Engineering

University of California, Los Angeles, 2019

Professor Samanvaya Srivastava, Chair

The phase behavior of particle-polyelectrolyte complexes was systematically studied using a model system comprising oppositely charged silica nanoparticles and poly(allylamine) hydrochloride (PAH) polycations. Phase behaviors of aqueous mixtures of silica nanoparticles and PAH were elucidated over a wide parameter space of particle and polyelectrolyte concentrations as well as solution pH. Trends in phase behaviors were analyzed to create a fundamental understanding of the fundamental properties that govern the complexation of these oppositely charged species.

The thesis of John Neilsen is approved.

Vasilios Manousiouthakis

Junyoung O. Park

Samanvaya Srivastava, Committee Chair

University of California, Los Angeles

2019

Contents

List of Figures

List of Tables

Acknowledgments

I would like to thank my family who has given me unconditional love and support throughout my whole life, I owe the whole my well-being to you. I would also like to thank my advisor, Professor Samanvaya Srivastava, who has been extraordinarily patient and supportive throughout my tenure at UCLA. I would not be here, were it not for his persistent support and dedication to my growth. I am extremely grateful for all I have learned from him. Lastly, I would like to thank my best friends and roommates Kelly and Nick, who have been by my side through thick and thin. I look forward to seeing the great things they will do.

Chapter 1

Introduction

Polyelectrolytes are a class of polymers in which significant fractions of monomers carry ionizable groups.[1,2] These polymer salts, polyacids or polybases (macro-ions), dissociate from their respective counter ions (micro-ions) in aqueous solutions. In dilute solutions, polyelectrolytes often assume rod like conformations due to the electrostatic repulsions between like-charged monomers.[3] In the presence of oppositely charged materials (polyelectrolytes, particles, surfaces, etc.), electrostatic interactions induce association, commonly referred to as complexation, resulting in materials with unique properties.[2,4] Polyelectrolyte complexes play vital and irreplaceable roles in biology, including the roles of DNA folding around histone proteins in chromatin.[5,6] At the same time, technological applications increasingly employ polyelectrolyte complexes in diverse settings ranging from drug delivery vehicles[7,8] to wastewater treatments.[9] Yet, owing to a complex interplay between electrostatic interactions, hydrophobic interactions and entropy, our understanding of the structure and properties of polyelectrolytes in solution and in assemblies is far from complete and continually developing.

1.1. Aqueous Particle-Polyelectrolyte Self-Assemblies

In this thesis, we investigate the interactions between cationic polyelectrolytes and negatively charged silica particles as a model system to delineate paradigms of self-assembly in aqueous dispersions of oppositely charged particles and polyelectrolytes. Particle-polyelectrolyte self-assemblies are omnipresent in both biological and technological realms, and have been

investigated through application based studies.[10,11] For example, particle-polyelectrolyte complexes have been used to template microcapsules and investigate the effect of polyelectrolyte flexibility in complex formation, but have never been studied systematically.[10,11] By employing a systematic design of experiments we seek to elucidate the effect of several of the key variables, including polyelectrolyte and particle concentration, solution pH and particle size, and how they affect the phase behavior of the particle-polyelectrolyte complexes.

1.2. Biological Significance

Particle-polyelectrolyte complexes are commonly encountered in biological settings involving complexation of proteins with polyelectrolytes and hetero-protein complexes. A ubiquitous example of such assemblies is the complexation of DNA with histone proteins. Chromatin is composed of DNA wrapped around histone proteins, which fold into fibers and self-assemble into large bundles.[6] This wrapping of DNA is primarily charge-driven as histones are positively charged proteins and DNA carries a net negative charge. The wrapping of DNA is extremely efficient, such that there is a 10,000 fold reduction in the length of the DNA strand.[6] This enables chromatin to store huge amounts of genetic information in tight spaces inside the nucleus. The complexation of DNA and histone proteins has an incredibly high level of specificity and packing efficiency; synthetic systems have never been able to replicate this packing efficiency.

1.3. Technological Applications

The unique structure and properties of these particle-polyelectrolyte assemblies enable their use in diverse applications. The most widely studied application for particle-polyelectrolyte

complexes is their utilization in polyelectrolyte complex micelles as stimuli-responsive drug delivery vehicles.[8] These assemblies can be designed to encapsulate and specifically deliver charged molecules like nucleic acids[7] and hydrophilic drugs[8] and deliver them *in vivo.* The assemblies achieve this followed by protecting the cargo from enzymatic degradation and mitigating off-target delivery and then spontaneously disassembling in targeted locations.[8] Kataoka and coworkers recently used gold nanoparticles as a templating device for these types of drug delivery vehicles.[7] The gold nanoparticle templated polyelectrolyte complex micelles showed improved size controls and circulation times.[7]

Polyelectrolyte-particle assemblies have also been shown as viable templates for microcapsule synthesis.[11,12] Kaufman and coworkers synthesized microcapsules in microfluidic devices by flowing water droplets containing high concentrations of charged particles through an organic phase containing high concentrations of oppositely charge polyelectrolytes. Complexation occurring between the charged particles and polyelectrolytes resulted in the formation of a shells on the surface of the droplets. After drying, these microcapsules retained their shape and allowed the controlled diffusion of fluids through the capsule walls.[11]

More recently, charged particle-polyelectrolyte complexes have been employed as chemical sensors. Cohen-Stuart and coworkers demonstrated the use of them as hydrophilic, biocompatible MRI contrast agents by incorporating iron and manganese particles into polyelectrolyte complex micelles. These sensors displayed significantly improved contrast effects in MRI scans of livers and kidneys.[13]

In this thesis, we present on the fundamental phase behavior of particle-polyelectrolyte complexes in an attempt to inform the design of particle-polyelectrolyte complex-based

materials. The arrangement of this thesis is as follows: Chapter 2 provides a detailed background on polyelectrolyte complexation and particle-polyelectrolyte complex self-assemblies. Chapter 3 includes the experimental design and procedures, the compilation and discussion of the experimental results. Lastly, chapter 4 includes a summary of the research and future research directions for this project.

Chapter 2

Background: Polyelectrolyte Complexation and Particle-Polyelectrolyte Self-Assemblies

When aqueous solutions of oppositely charged polyelectrolytes are mixed together, electrostatic attractions and counterion release conspire to result in an associative phase separation of the polyelectrolytes, termed as polyelectrolyte complexation.[14-16] The resulting phases consist of a polyelectrolyte-rich phase termed, polyelectrolyte complex coacervate and a polyelectrolyte-deplete supernatant phase.

The change in free energy of the phase-separation process, $\Delta G = \Delta H - T\Delta S$, has contributions from both the electrostatic interactions (ΔH) and entropy gains from counterion release accompanying complexation of polyelectrolyte chains (ΔS). In dilute polyelectrolyte solutions, counterions form a shell around the polyelectrolyte chains.[3] Upon complexation, the oppositely charged polyelectrolytes neutralize each other, releasing the counter-ions. The counter-ion release results in significant increase in the total configurational entropy of the system that always contributes favorably towards complexation and subsequent phase separation.[1] The electrostatic enthalpy change, however, can either contribute to or hinder complexation.[1] While the electrostatic interaction between oppositely charged polyelectrolytes is always attractive, a very charge dense polyelectrolyte will have a large concentration of counter-ions near the chain and this can result in the counter-ion clouds screening the interactions between polyelectrolytes, making complexation less favorable.[1]

2.1 The Voorn-Overbeek Theory

The phenomena of charge driven complexation was first studied by Bungenberg De Jong with gelatin/gum arabic mixtures in 1929.[17] The first theoretical description of this phenomena, however, was proposed by Voorn and Overbeek in 1956.[18] The Voorn-Overbeek (VO) theory, as it is commonly referred to in the literature, provided both a qualitative description of the phenomena as well as a quantitative framework for determining the conditions for complexation and the compositions of the resulting phases. The theory approximates the entropy change of the mixture using a Flory-Huggins lattice model and estimates the enthalpy change using a Debye-Hückel description of the electrostatic attractions between the charged species. The VO theory is simple and effective, yet incomplete: various assumptions that are inherent in the theory include ignoring chain connectivity of charges, treating all molecules in the polyelectrolyte, salt and solvent with equal molecular sizes and neglecting long range electrostatic interactions. The shortcomings of those assumptions have been shown to increasingly render the theory incapable of capturing finer details of polyelectrolyte complexation.[19]

In its simplest form, the VO theory assumes equivalent charge densities and chain lengths for the two polyelectrolytes, the polyelectrolytes (and correspondingly the counter-ions) are present in equal concentrations, and the molecular volume of the both kind of monomers, both kind of counter-ions and water are all the same.[18] In a "2-component" symmetrical system, only polyelectrolytes and water are considered. The total free energy is described given by:[18]

$$f = \frac{F}{NkT} = -\alpha(\sigma\phi_p)^{\frac{3}{2}} + (1-\phi_p)ln(1-\phi_p) + \frac{\phi_p}{N} ln\left(\frac{\phi_p}{2}\right)$$

Here, N, ϕ_p and σ refer to the polyelectrolyte degree of polymerization, volume fraction and charge density, respectively. α refers to the interaction parameter, which is an approximate measure of the electrostatic attractions between charged groups. An analysis of the free energy function at fixed N and σ reveals the ϕ_p window for phase separation as well as the compositions of the respective phases, as shown in Figure 2.1. Regions where phase separation occurred were identified as the regions where the free energy as a function of total polyelectrolyte concentration was concave, $\partial^2 f / \partial \phi^2 < 0$.

In the treatment of a "3-component" system, counter-ions are included in addition to the polyelectrolytes and water, although equal ionic strengths of the two polyelectrolytes and the two salt ions, respectively, are still maintained. The addition or removal of salt has considerable

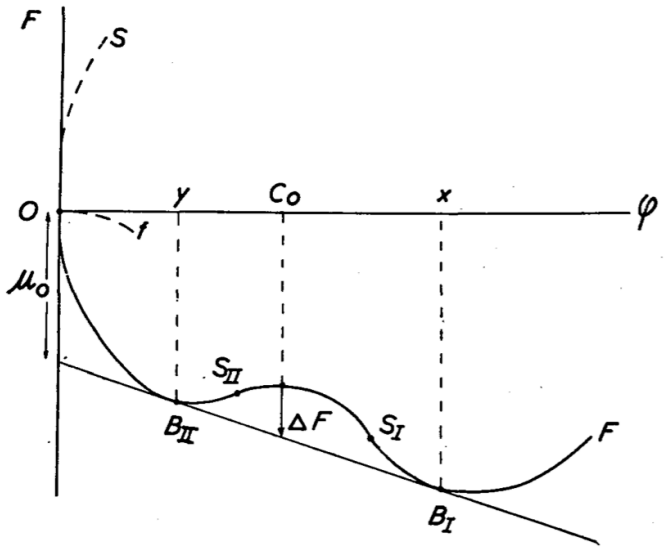

Figure 2.1: Total free energy for a system of symmetric polyelectrolytes with polyelectrolyte concentration, φ. Common tangent construction was employed to determine the total polyelectrolyte concentration in the resulting phases, (x = coacervate, y = supernatant) following phase separation, with B_I and B_{II} denoting the state of the system following binodal decomposition. S_I and S_{II} represent the state of the system following spinodal phase separation. Adapted with permission from (Voorn and Overbeek, 1956). Copyright © (1956) Wiley-VCH Verlag GmbH and Co.

effects on the complexation conditions for the system. As previously stated, an increase in salt concentration can screen the electrostatic interactions between the polyelectrolytes and also reduce the entropic gain from counter-ion release, diminishing the overall propensity for complexation. The total free energy expression is modified to account for counter-ion (salt) concentrations as

$$f = \frac{F}{NkT} = -\alpha\left(\phi_s + \sigma\phi_p\right)^{\frac{3}{2}} + \phi_s ln\left(\frac{\phi_s}{2}\right) + \frac{\phi_p}{N} ln\left(\frac{\phi_p}{2}\right) + \left(1 - \phi_s - \phi_p\right) ln\left(1 - \phi_p - \phi_p\right)$$

Here, ϕ_s refers to the counter-ion concentrations. At equilibrium, the electrochemical potentials of each component must be equal in both the phases. Thus, a system of three equations with four unknowns (ϕ_p and ϕ_s in each phase, ϕ_p^I, ϕ_s^I, ϕ_p^{II} and ϕ_s^{II}) can be deduced. By fixing one of these parameters (say ϕ_s^{II}), the other three parameters (ϕ_p^I, ϕ_s^I and ϕ_p^{II}) can be

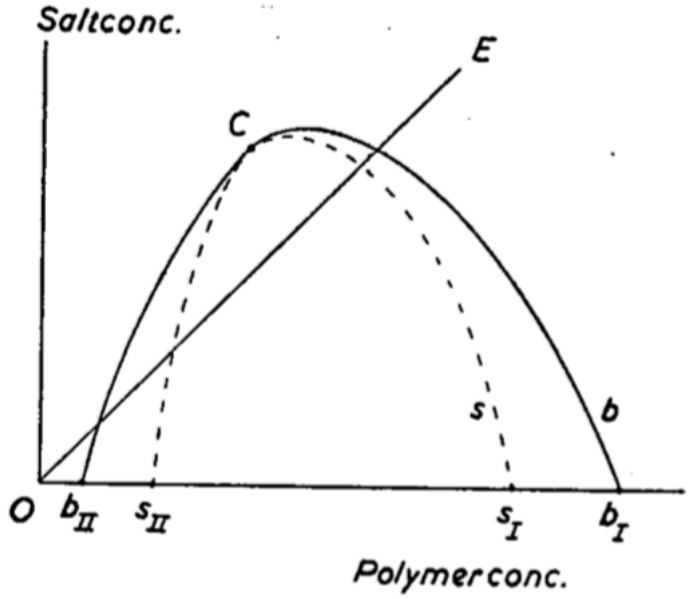

Figure 2.2: Binodal (*b*) and spinodal (*s*) phase envelops depicted in the polymer concentration-salt concentration space for a 3-component system. Systems with compositions within the two-phase envelope phase separate. *OE* represents the line of equal salt and polymer concentrations. Reprinted with permission from (Voorn and Overbeek, 1956). Copyright © (1956) Wiley-VCH Verlag GmbH and Co.

obtained, thus determining the compositions of both phases. Performing those calculations over a range of ϕ_s^{II} results in the complete phase diagram as depicted in Figure 2.2. While the VO theory provides a simple and powerful framework for analyzing coacervate systems, it's limitations are well known.[19] It should be noted that the VO theory predicts that salt concentration will be greater in the coacervate phase than in the supernatant. Recent studies have shown that this is not the case and in fact the supernatant will generally have a higher salt concentration than the coacervate.[20] This discrepancy arises from the fact that the VO theory doesn't take into account excluded volume interactions and ignores chain connectivity of charges. These interactions expel ions from the polyelectrolyte complex increasing the entropy of the system and decreasing the volume of the coacervate.[19]

Other theories have attempted to expand on the VO theory by making additional contributions to the free energy function. For example, the random phase approximation adds the cooperative electrostatic contributions of polyelectrolyte charges being connected by the chains.[19] Computer simulations have played a defining role in determining both the details of the molecular structure and the bulk properties of polyelectrolyte complexes. Molecular dynamics simulations are typically used for analyzing single chain, two chain and chain/particle structures[19-23] while mean-field and Monte-Carlo methods are typically used for predictions of bulk properties.[1,24-27]

2.2. Particle-Polyelectrolyte Complex Self-Assemblies

Polyelectrolyte complexation has received significant attention in the recent years as a new paradigm for materials design. The interactions and complexation of polyelectrolytes with

oppositely charged macro-ions (charged nanoparticles, proteins, dendrimers, etc.) are equally versatile and commonly found in nature. One such example of DNA wrapping around histone proteins to form chromatin was discussed in Chapter 1.[6] However, this class of assemblies has not received adequate attention yet, owing to the complexities of the biological conformations. Now, advances in polymer synthesis and materials characterization techniques and computer simulations have enabled systematic investigations of these diverse assemblies.[19-21]

Electrostatic attractions are still the primary driving force for inducing complexation of polyelectrolytes with oppositely charged macro-ions. However, there are several key differences between polyelectrolyte complexation and particle-polyelectrolyte complexation. Polyelectrolyte complexation is generally driven by a combination of enthalpic gains from electrostatic attraction and entropy gains from counter-ion release.[1] In the case of particle-polyelectrolyte complexation, the release of counter-ions contributes less to the overall entropy change owing to the weaker localization of counterions near the particle surfaces. However, depletion interactions contribute majorly towards the entropy gains. When particles come into contact, the volume excluded by the particles decreases, making more volume available for the surrounding molecules (solvent, polyelectrolytes), thus contributing to the translational entropy of both the solvent and the polyelectrolyte chains and thermodynamically favoring complexation.[28]

2.3. Key Parameters Influencing Particle-Polyelectrolyte Complexation

The structure, properties and function of particle-polyelectrolyte complexes can be best understood by gaining an in-depth understanding of the influence of the key parameters

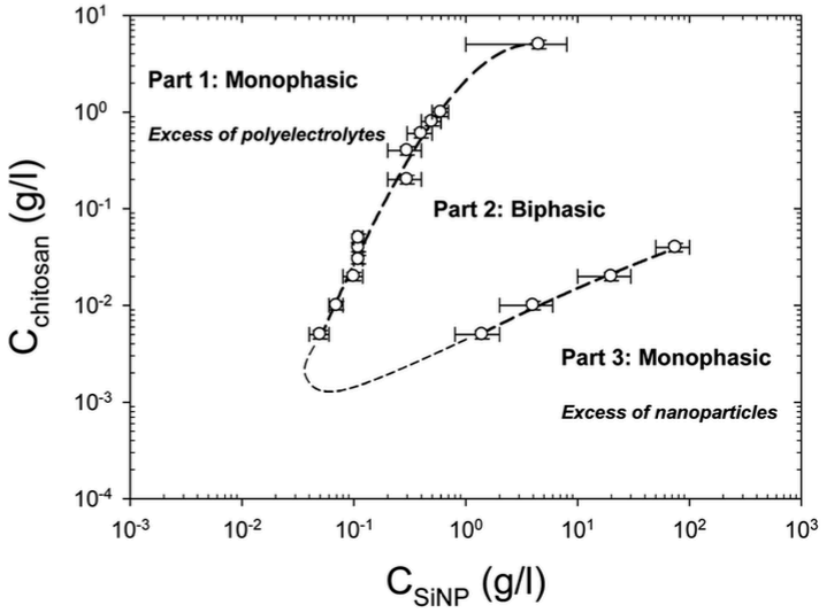

Figure 2.3: Experimental phase diagram for aqueous mixtures of chitosan and silica depicting monophasic and biphasic regions in the particle concentration (C_{SiNP})-polymer concentration ($C_{chitosan}$) space at pH 4.5. Reprinted with permission from (Shi et al., 2013). Copyright © (2013) Royal Society of Chemistry.

including the concentration of the constituents, their charge densities and comparisons of the relevant length scales associated with the constituents. Generally, for a mixture of oppositely charged particles and polyelectrolytes, a two-phase region can be observed in the appropriate concentration windows, as illustrated in the phase diagram depicted in Figure 2.3 for chitosan-colloidal silica complexes.[10] It is important to note that the two phases generated by phase separation are starkly different from either of the monophasic solutions and comprise a dense phase containing high concentrations of both particle and polyelectrolytes and a supernatant phase depleted in both the constituents. Particle charge can have a significant effect on the ability of polyelectrolyte chains to adsorb to the particle surface, as well as their interactions with other particles. For weakly charged particles, short-range attraction due to the depletion interactions can outcompete long-range inter-particle electrostatic repulsion, resulting in

particle aggregation. As particle charge density increases, inter-particle interactions become progressively repulsive, increasing the extent of chain adsorption onto the particle surfaces and favoring complexation.[28] For example, studies by Obermayer and coworkers on protein-polyelectrolyte complexes demonstrated that supercharging of proteins was necessary to achieve complexation with various polyelectrolytes.[29]

The strength of the electrostatic interactions (between particles and polyelectrolytes, between particles and other particles, between monomers on the same chain and between monomers on different chains) can be tuned by varying salt content in the solution or the pH of the solution. Interestingly, it has been shown through both experiments and simulations that complexation between strongly charged particles and polyelectrolytes is maximal at intermediate salt concentrations.[22,26] At very low salt concentrations, the electrostatic intra-chain repulsion hinders absorption of the chains on the particle surfaces, preventing complexation.[26] Conversely, at very high salt concentrations, the electrostatic interactions between particle and polyelectrolyte are strongly screened and therefore results in desorption of the polyelectrolyte chain and disruption of the complex.[26,30,31] Similarly, variations of solution pH can be harnessed to modulate the degree of charge in both polyelectrolytes and nanoparticles, thus influencing the magnitude of electrostatic interactions.[21,32]

The influence of chain length and particle size on the formation and structure of particle-polyelectrolyte complexes are inherently intertwined, and can be described in terms of the ratio between the chain's contour length and particle diameter, β. At high β values, polyelectrolytes can fully cover the particle surfaces and still have unadsorbed tails extending from the surface.[30] Conversely, at very low β values, the phenomena is better described by the adsorption of

particles on a polyelectrolyte chain and the conformations are not very different than the normal chain conformations.[6] Additionally, in presence of long chains, multiple particles can also be bridged by individual polyelectrolyte chains, resulting in the phenomena known as polyelectrolyte bridging.[25] Bridging typically causes particles to cluster and subsequently, at adequate cluster density, phase separation. In special cases, bridging can also result in formation of unique self-assembled structures, including glassy phases, nanorods and gels.[10,25] In general, increasing chain length expands the phase diagram and allows for a wider range of compositions that lead to complexation.[19,30] Another important variable for controlling the structure of particle-polyelectrolyte complexes is polyelectrolyte flexibility. Often quantified in terms of the persistence length, flexibility impacts the efficiency of chain adsorption on the particle surfaces.[10] Generally, increasing stiffness decreases the ability of a polyelectrolyte chain to adsorb on the surface of a particle.[33] Increasing polyelectrolyte stiffness can lead to various solenoid conformations at sufficiently large chain lengths.[23] For semi-flexible polyelectrolytes in excess of charged nanoparticles, polyelectrolytes can also take the form of nano-rods.[10] The influence of the interplay between chain length and salt concentration and between chain length and chain flexibility, respectively, on the structure of the particle-polyelectrolyte complexes were described by Schiessel et al. by employing molecular dynamics simulations. The key results from these studies are depicted Figure 2.4. In both the cases, increasing chain length at constant salt concentrations and persistence length, respectively, resulted in an increase in the solenoid number of loops. As illustrated in Figure 2.4 (a), decreasing salt content lead to an increase in the electrostatic attraction between particles and polyelectrolytes, resulting in a wrapped state where the polyelectrolyte chains partially or fully collapsed onto the particle

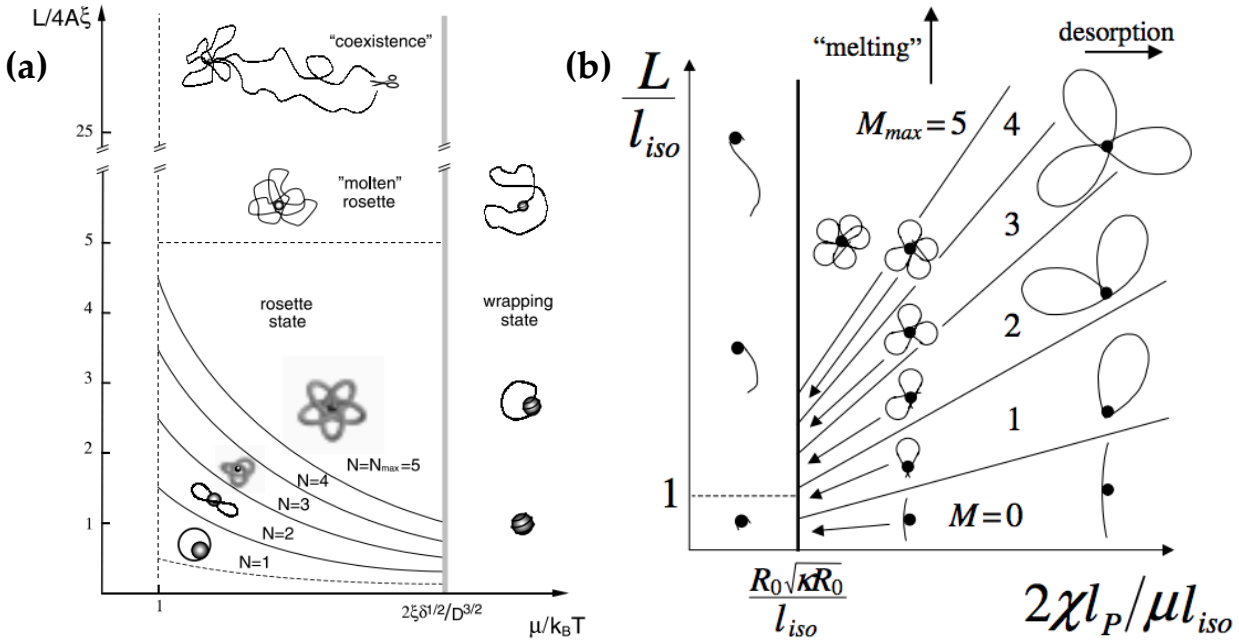

Figure 2.4: Results of molecular dynamics simulations of a single polyelectrolyte chain interacting with a charged nanoparticle with increasing chain lengths. The y-axis of both figures represents chain length. The x-axis of figure (a) represents adhesion energy which is inversely proportional to salt concentration. The x-axis of figure (b) refers to the polymer persistence length which is proportional to chain stiffness. The different configurations are characterized by the number of loops in the solenoid conformations determined by number of contacts of a chain with the particle surface. Adapted with permission from (Schiessel et al., 2000) and (Schiessel, 2003), respectively.

surface. Similarly, as depicted in Figure 2.4 (b), increasing chain stiffness did not change the shape of the solenoids but increased the chain length necessary to create similar structures. Increasing the stiffness sufficiently lead to desorption of the polyelectrolyte from the particle. Finally, in both cases, increasing the chain length sufficiently resulted in a molten configuration where the conformation of the polyelectrolyte chain was not dependent on the presence of particle. In this case, the system was best be described by the adsorption of particles on the polyelectrolyte chains.

2.4 Characterization Techniques

Structural characterization of particle-polyelectrolyte complexes can be achieved using diverse techniques. Optical and electron microscopy can enable visualization of the complex microstructures. Static and dynamic light scattering can allow for the assessment of the hydrodynamic size and molecular weights of self-assemblies. Small angle neutron and x-ray scattering can provide information about the shape and size of the assemblies, as well as about the particle distribution in the self-assembled complexes. Techniques as simple as turbidimetry can also provide valuable information about the nature of the assemblies in solution. Typically, it is a combination of these techniques are employed to gain a comprehensive structural description of the complexes.

For instance, determination of particle distribution in the self-assembled structures requires a combination of characterization approaches. Optical microscopy will be highly limited owing to the solution phase of the complexes and the small sizes of the particles. Cryo-TEM may allow for examination of these structures in solution by flash freezing and imaging the samples *in situ*.[11] However, it requires preparation of thin films of samples and will only provide information over a small length-scale of the sample. Light scattering can provide the hydrodynamic radius of the assemblies in solution, which can in turn be related to the degree of compaction of the complexes. Small radii of the assemblies imply good dispersion of particles while large radii are indicative of particle aggregation. Small angle x-ray scattering (SAXS) and small angle neutron scattering (SANS) can also provide highly useful information about the distribution of the particles. Small angle scattering can probe structural features at length scales on the order of 1 to 100 nm.[10] This allows access to the fractal regime, the determination of

which provides information about how densely the material is compacted, as well as particle distribution functions and inter-particle distances.

2.5. Summary

There have been isolated experimental reports on the structure and properties of particle-polyelectrolyte complex self-assemblies over the last 15 years.[10,11,34] A comprehensive understanding of the fundamental phase behavior of these systems, however, is still elusive. Some generalized conclusions about the effects of different parameters have been presented[10], but most of the effects have been studied on poorly characterized systems such as polyelectrolytes with broad molecular weight distributions and polydisperse particles. Furthermore, predictions from theoretical treatments and computer simulations have often not been explicitly verified with experiments. Therefore, detailed experimental investigations of the structure and properties of particle-polyelectrolyte complex self-assemblies with meticulous variation of the system parameters are imperative for enhancing the fundamental understanding of these systems. These investigations are expected to expand the scope of applications of particle-polyelectrolyte complexes in areas ranging from water purification to additive manufacturing and from protein purification to gene and drug carriers.

Chapter 3

Turbidimetric Mapping of the Particle-Polyelectrolyte Phase Space

The studies detailed in Chapter 2 highlight many interesting and unique phenomena found in particle-polyelectrolyte complexes. However, none of them provide a clear and unified picture for how the key parameters influence the fundamental phase behavior of these systems. We seek to understand this behavior by mapping phase diagrams of particle-polyelectrolyte complexes over a wide parameter space using a model particle-polyelectrolyte mixture.

3.1. Initial Investigations

When complexation between oppositely charged particles and polyelectrolytes leads to the formation of aggregates that are large enough to scatter light, distinct quantifiable changes in solution cloudiness occur that are assessable via turbidimetry. We establish the viability of our methodology by direct comparisons with published results[10] on the phase boundaries of particle-polyelectrolyte complexes. These complexes consist of mixtures of positively charged bio-polyelectrolyte chitosan and negatively charged colloidal silica at pH 4.5, and the structure is ascertained by SANS experiments. The resulting phase diagram is shown in Figure 3.1. Our experimental results are superimposed on the published results, with red and green filled circles corresponding to uniform and phase-separated systems, respectively. A strong qualitative agreement between the reported phases boundary from SANS experiments and our turbidimetry data was observed, establishing the robustness of our experimental approach.

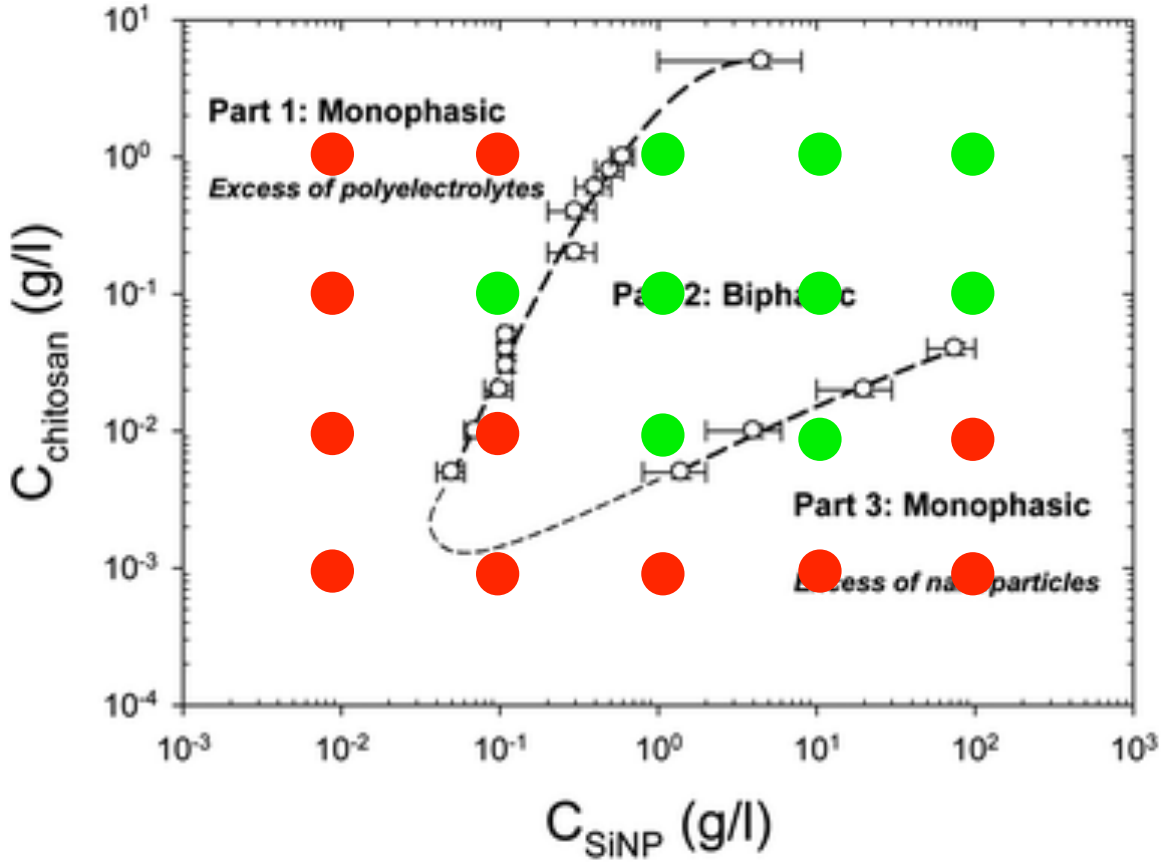

Figure 3.1: Phase diagram for silica-chitosan mixtures reported by Shi and coworkers (Shi et al., 2013) using small angle neutron scattering. Superimposed on the figure are turbidimetry results from our investigations. Red dots indicate no significant change in the overall solution turbidity. Green dots represent ≥50% change in the overall solution turbidity. Adapted with permission from (Shi et al., 2013). Copyright © (2013) Royal Society of Chemistry.

3.2. Parameter Space

We employed aqueous dispersions of colloidal silica and poly(allylamine) hydrochloride (PAH) as our model particle and cationic polyelectrolyte, respectively. Our investigations were conducted with three SiO_2 particles with average diameters of 7, 12, and 22 nm, respectively, and PAH of molecular weight 17,500 g/mole. The key parameters investigated in our studies were concentrations of both polyelectrolyte and particle, particle sizes, and the solution pH. The polyelectrolyte concentration ranges from 0.001 g/L to 10 g/L and the particle concentration

ranges from 0.01 g/L to 100 g/L. The other key parameter we sought to control was the solution pH, that in turn enabled control of the degree of ionization of the PAH chains and the charge density of SiO_2 particles. Upon decreasing pH, PAH progressively becomes more ionized while colloidal silica becomes less charge dense. The degree of ionization of PAH can be calculated using the Henderson-Hasselbach equation:

$$pH = pK_a + log\left(\frac{[A^-]}{[HA]}\right)$$

pKa, also known as the acid dissociation constant, is a quantitative measure of the strength of an acid in solution. While the charged groups on colloidal silica do not have explicit pKa values, the charge state of these particles can be quantitatively assessed using zeta potential measurements.[32] We chose the pH values of 4.5, 7.4 and 9.0 because this would allow us to study the differences in the charged state of both polyelectrolyte and particle. The effects of pH on the particles and polyelectrolytes are summarized in the Table 3.1.

Table 3.1: Polyelectrolyte degree of ionization and particle zeta potentials as a function of solution pH. Three pH regimes were identified – pH 4.5: very high polymer charge density, low particle charge; pH 7.4 high polymer charge density, high particle charge; pH 9.0 Low polymer charge density, very high particle charge. The particle zeta potential values are from (Kobayashi et al., 2005).

pH	**Polyelectrolyte Degree of Ionization (% ionized)**	**Particle Zeta Potential (mV)**
4.5	>99.9%	~15mV
7.4	92%	~30mV
9.0	42%	~35mV

3.3. Materials and Methods

Poly(allylamine) hydrochloride was purchased from Sigma-Aldrich and had an average molecular weight of 17,500 g/mol. Silica suspensions (Ludox SM30, HS40 and TM50) were also purchased from Sigma Aldrich. SM30 has an average particle diameter of 7 nm and an average surface area of 350 m^2/g. HS40 has an average particle diameter of 12 nm and an average surface area of 220 m^2/g. TM50 has an average particle diameter of 22 nm and an average surface area of 140 m^2/g. The pH 4.5 buffer was a 0.2 M acetic acid and 0.3 M sodium acetate solution in deionized (DI) water. The pH 7.4 buffer was a 1M Tris-base and 0.84M HCl solution in DI water. The pH 9.0 buffer was a 1M Tris-base and 0.114M HCl solution in DI Water.

Solution turbidity was measured using a Tecan Infinite 200 Pro Microplate reader. The plates used were Corning Costar brand 96-well plates. 1.5 ml of each sample was prepared in 2 ml Eppendorf tubes and thoroughly vortexed to ensure mixing. 100 μL specimens from each sample were subsequently pipetted into the individual wells of the well-plates. Turbidimetry experiments were operated at an absorbance of 500 nm and the measurements were taken in a 3x3 grid over each well and averaged to obtain the overall sample turbidity.

3.4. Phase Diagrams

Figure 3.2 shows a representative phase map for silica-PAH mixtures for 7 nm silica particles at pH 7.4. Solution turbidity was measured with varying particle and polyelectrolyte concentrations, with each dot on the phase map corresponding to an experiment. The three regions depicted in the phase diagram are colored in blue, red and green. The red regions represent compositions wherein complexation resulted in an increase of >50% in the solution

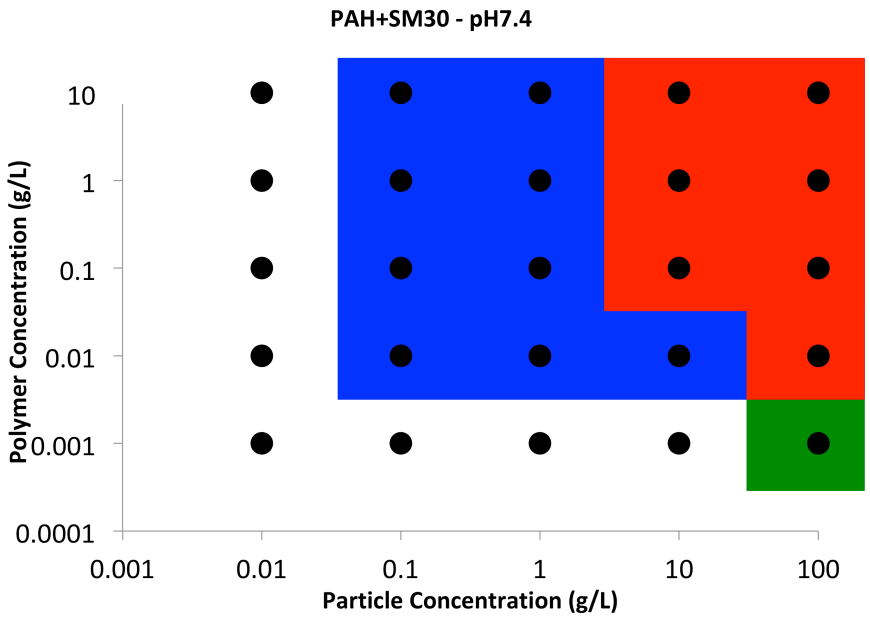

Figure 3.2: Turbidimetric phase diagram for aqueous mixtures of PAH and 7nm silica particles at pH 7.4. Black dots correspond to experimental composition investigated. Red regions represent compositions wherein complexation resulted in an increase of >50% in the solution. The blue regions represent compositions where flocs were observed in otherwise clear solutions, but there were no significant changes in the solution turbidity. The green regions represent compositions where the complex volume of the solution reached 100%, which was identified as a gel.

turbidity. In various particle-polyelectrolyte solutions, miniscule flocs were identified upon close visual inspection. Owing to their small size, however, these flocs did not contribute towards overall solution turbidity. The blue regions represent compositions where flocs were observed in otherwise clear solutions, but there were no significant changes in the solution turbidity. The green regions represent compositions where the complex volume of the solution reached 100%, which was identified as a gel.

Figure 3.3 depicts all the phase diagrams produced for different particle sizes and at different solutions pH values. Various trends can be qualitatively identified from these phase mappings, with noticeable effects of particle size and pH on the overall solution phase behaviors. The phase diagrams of mixtures with SM30 particles (smallest particles, 7 nm

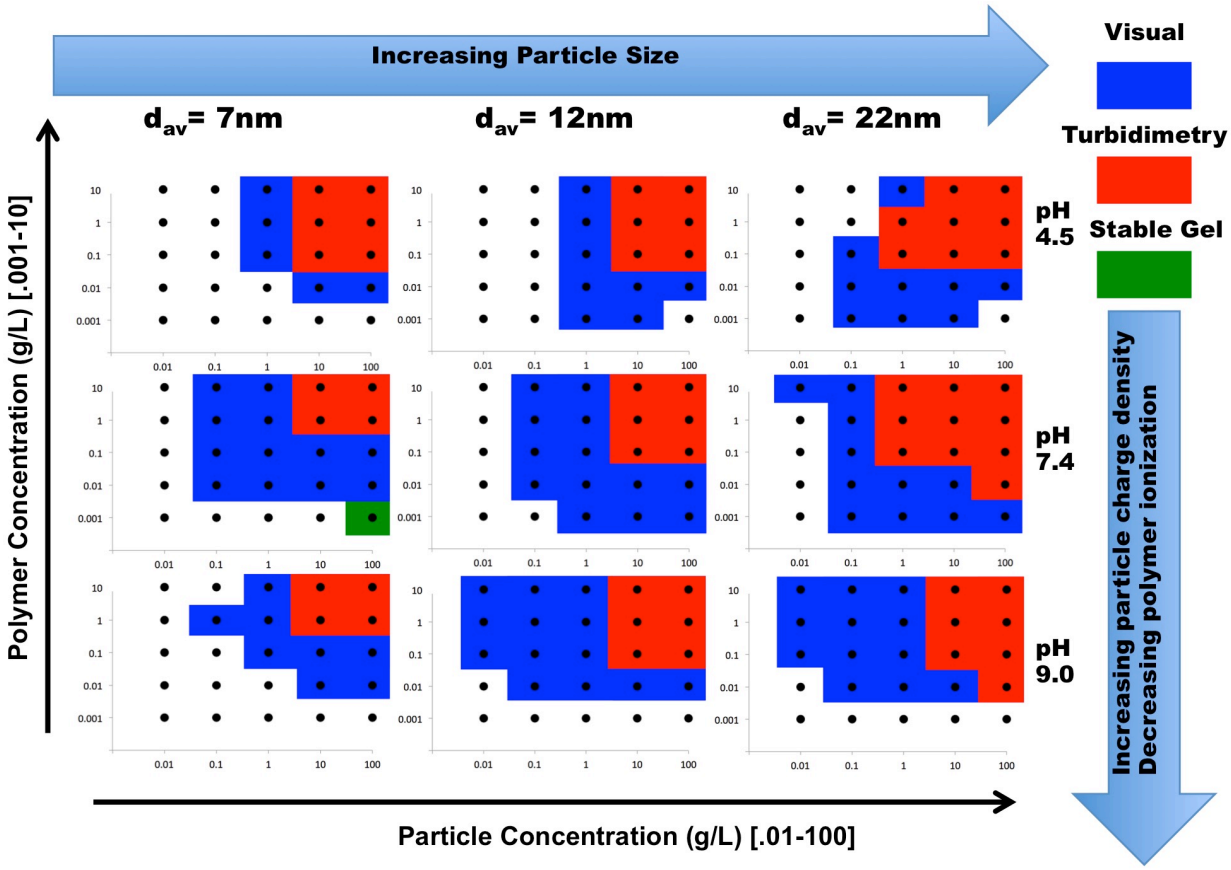

Figure 3.3: Turbidimetric phase diagram for aqueous mixtures of PAH and silica particles at three different silica particle sizes and at three different solution pH conditions. Black dots correspond to experimental composition investigated, with polymer concentrations ranging from 0.001-10 g/L and particle concentrations ranging from 0.01 - 100 g/L. Red regions represent compositions wherein complexation resulted in an increase of >50% in the solution. The blue regions represent compositions where flocs were observed in otherwise clear solutions, but there were no significant changes in the solution turbidity. The green regions represent compositions where the complex volume of the solution reached 100%, which was identified as a gel. Out of the total 225 unique concentration, pH and particle size samples, only one exhibited a stable gel phase.

diameter) exhibited the smallest biphasic $C_{particle}$-$C_{polymer}$ windows at all solution pH conditions tested in our experiments. The biphasic windows for TM50 particles (largest particles, 22 nm diameter) were similar, albeit slightly larger, as compared to the corresponding windows for the HS40 particles (intermediate particles, 12 nm diameter). Thus, it can be surmised that larger particles have a greater tendency to form phase-separated complexes with polyelectrolytes at

lower particle concentrations. Solution pH also affected the size of the biphasic windows noticeably. At pH 4.5, the window for phase separation were markedly smaller than those at pH 7.4 or 9.0 for all three particles sizes. There are some differences in the size of the phase windows between the 7.4 and 9.0 pH samples, but not enough to make general conclusions. Interestingly, an apparent tradeoff between the degree of ionization and concentrations required for complexation was observed, for particles as well as polyelectrolytes. In the high polyelectrolyte and low particle charge case (4.5 pH), complexes formed at very low polyelectrolyte concentrations, but much higher particle concentrations were required for complexation. Conversely, at high particle and low polyelectrolyte charge (9.0 pH), complexes formed readily at very low particle concentrations but required a moderate concentration of polyelectrolytes.

The volume of the complexes that formed upon phase separation also exhibited interesting trends. With increasing particle concentrations, the volume fraction of the complex phase increased. Conversely, the volume fraction of the complexes decreased upon increasing the polyelectrolyte concentrations. These trends were preserved over all particle sizes and pH conditions. Furthermore, larger particles led to smaller complex volumes at comparable particle and polyelectrolyte concentrations and charges. While this trend could only be reliably observed for samples with sufficient complex volume fractions to be visually compared (i.e. particle concentrations ≥ 1 g/L), the trend was preserved over all solution pH values. It should be noted that formation of a stable percolated gel phase (i.e. 100% complex volume fraction) was observed at conditions corresponding to maximum complex volume fractions upon combining these trends – smallest particles, highest particle concentration, lowest

polyelectrolyte concentration and pH 7.4 which had the combined highest number of ionized groups. Another interesting visual observation was the appearance of the glassy complex phases at very high polyelectrolyte concentration. While typical phase separated systems had complexes appearing as milky white dense flocs, the glassy complexes had translucent flakey appearance. This occurred for all particle sizes and solution pH values investigated.

3.5. Discussion

The pH of the solution influences the charge on both the polyelectrolyte and the particles, and therefore influences the phase behavior profoundly. The smallest biphasic windows existed for pH 4.5 systems which correspond to the lowest particle and the highest polyelectrolyte charges. It is important to note that the total number of charged groups differs between particles and polyelectrolytes per mass of each constituent. The average number of charges per gram of PAH added can be estimated as $e/m = INN_{Av}/M_w$, where e/m is the number of charges per gram, I is the degree of ionization, N is the average chain length, N_{Av} is the Avogadro number and M_w is the average molecular weight. Similarly, the charge mass density of colloidal silica particles can be found using as $e/m = \sigma_0 a_s$, where e/m is the number of charges per gram, σ_0 is the electro-kinetic surface charge density and a_s is the average surface area. The values for average surface areas were taken from the manufacturer and electro-kinetic surface charge density values were based on reported values as a function of pH.[35] Based on these simple calculations, the difference in the total number of charges per gram for polyelectrolytes is typically two orders of magnitude higher than the particles. It would follow that the phase behavior of the mixtures would be less dependent on the degree of ionization of the polyelectrolytes. When the

polyelectrolytes are at their lowest degree of ionization (42% for pH 9.0), there are still a greater number of positively charged groups per mass than negatively charged groups. This would imply that the charge on the particles is the limiting parameter for complexation. This hypothesis agrees with the observation that at pH 4.5, where the particle charge density was the lowest, a higher particle concentration was required for complexation.

The effect of particle size on the phase behavior of the complexes can be interpreted by realizing that, at the same particle concentrations, smaller particles will have larger total particle surface area available for complexation. Thus, more polyelectrolyte chains will be required to achieve similar degrees of surface coverage and complexation.

The trends influencing the volume of the complex phase can also be argued to depend significantly on the charge on the particles and the associated interparticle repulsive interactions. Complex volume increases as particle concentration increases, resulting from increasing inter-particle repulsion. Increasing polyelectrolyte concentration, conversely, leads to more polyelectrolyte chains adsorbing onto the particles and thus screening the inter-particle repulsion. The effect of particle size on the complex volume may also be elaborated in the same vein; smaller particles have larger surfaces area and concomitantly more surface charge per unit volume, resulting in stronger inter-particle repulsion and larger complex volumes.

Figure 3.4 represents a theoretical phase diagram of charged particle polyelectrolyte mixtures.[25] In the phase diagram, the region called polyelectrolyte-bridged (PE-bridged) clustering zone is a region where each polyelectrolyte chain is adsorbing on two or more charged particles. Polyelectrolyte bridging can lead to particle clustering which causes phase separation; which we refer to as complexation phase formation. The region termed meta-stable

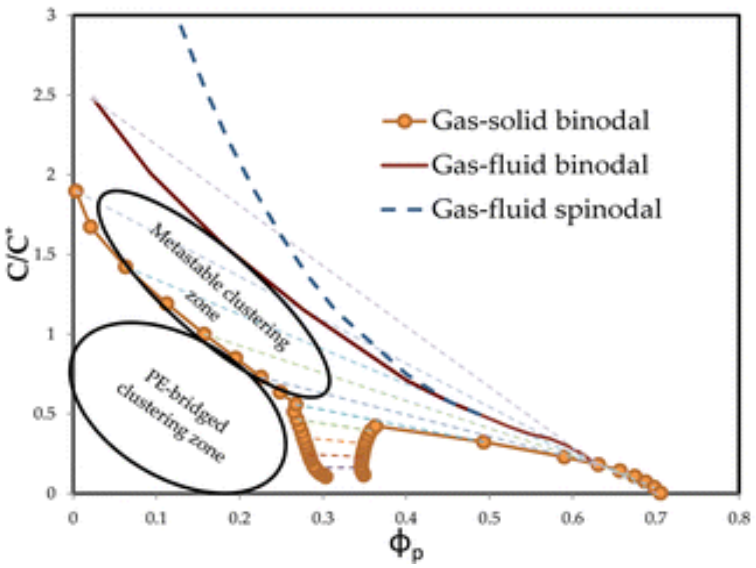

Figure 3.4: A theoretical phase diagram for particle-polyelectrolyte complexes. The x-axis represents the volume fraction of the particle. The y-axis represents the polyelectrolyte concentration normalized by overlap concentration. PE-bridged clustering zone and metastable-clustering zones are clearly identified.

clustering zone, which occurs at high polyelectrolyte and moderate particle concentrations, was characterized by a "dynamically arrested glassy phase". The glassy complexes observed in the experiments at very high polyelectrolyte concentrations agree with the theoretical description.[25]. These phases were understood to arise from the strong adsorption of many polyelectrolyte chains onto particles, leading to dense clustering where particles were unable to rearrange their configurations.

Chapter 4

Conclusions

We have investigated the influence of a few of the many parameters that affect particle-polyelectrolyte complexation. In addition, there are various additional characterizations that are required to achieve a comprehensive understanding of structure of these particle-polyelectrolyte mixtures. For instance, the influence of chain properties, length and stiffness, on complexation requires detailed investigation. Many theoretical treatments of the problem have discussed the effect of chain length in great detail and would enable intriguing theoretical-experimental comparisons.[21,22] Increased chain length could lead to even greater polyelectrolyte bridging effects with a single chain being able to adsorb onto an increased number of particles. It would be interesting to see if this would cause glassy phases to appear at even lower polyelectrolyte concentrations due to a greater degree of kinetic hindrance. Chain flexibility is known to affect polyelectrolyte complex phase behavior.[2] Numerous simulations have also studied the effect of chain flexibility for models of a single macro-ion interacting with a polyelectrolyte, but none have looked at how this parameter effects the overall phase behavior of particle-polyelectrolyte complexes.[10,23,33] The influence of particle size also needs to be investigated in further detail. While the experimental sets have already spanned three different particle sizes, the difference between the surface areas is only a little more than two-fold. Increasing the average particle diameter to ~100 nm would create a difference of over two orders of magnitude in particle surface area, which would undoubtedly provide deeper insights.

More extensive characterizations of the complex structure are also necessary for gaining a better understanding of these systems. Thermo-gravimetric analysis must be employed to ascertain the compositions of the complexes and the supernatants to determine excess polyelectrolyte or particles in the supernatant after complexation. Cryo-TEM would be particularly effective in understanding the underlying structure of the complex clusters. Colloidal silica particles are easily visualized using TEM and by cryogenically freezing the particles in place, one could study the structure *in situ* of these particle-polyelectrolyte complexes. The gel phase reported for one set of parameters can be important for design of self-assembled materials and warrant further investigation including other sets of compositions that lead to the gel formation and the rheology investigations of the gels as a function of concentration, pH and other relevant parameters. Overall, the experiments reported here are expected to serve as a nucleus for future work.

References

(1) van der Gucht, J.; Spruijt, E.; Lemmers, M.; Stuart, M. A. C. Polyelectrolyte Complexes: Bulk Phases and Colloidal Systems. *Journal of Colloid And Interface Science* **2011**, *361* (2), 407–422.

(2) Marciel, A. B.; Chung, E. J.; Brettmann, B. K.; Leon, L. Bulk and Nanoscale Polypeptide Based Polyelectrolyte Complexes. *Advances in Colloid and Interface Science* **2016**, 1–12.

(3) Colby, R. H. Structure and Linear Viscoelasticity of Flexible Polymer Solutions: Comparison of Polyelectrolyte and Neutral Polymer Solutions. *Rheol Acta* **2009**, *49* (5), 425–442.

(4) Stuart, M. A. C.; Huck, W. T. S.; Genzer, J.; Müller, M.; Ober, C.; Stamm, M.; Sukhorukov, G. B.; Szleifer, I.; Tsukruk, V. V.; Urban, M.; et al. Emerging Applications of Stimuli-Responsive Polymer Materials. *Nature Materials* **2010**, *9* (2), 101–113.

(5) Dubin, P. L.; Ross, T. D.; Sharma, I.; Yegerlehner, B. E. Coacervation of Polyelectrolyte-Protein Complexes. In *Ordered Media in Chemical Separations*; ACS Symposium Series; American Chemical Society: Washington, DC, 2009; Vol. 342, 162–169.

(6) Schiessel, H. The Physics of Chromatin. *J. Phys.: Condens. Matter* **2003**, *15* (19), R699–R774.

(7) Kim, H. J.; Takemoto, H.; Yi, Y.; Zheng, M.; Maeda, Y.; Chaya, H.; Hayashi, K.; Mi, P.; Pittella, F.; Christie, R. J.; et al. Precise Engineering of siRNA Delivery Vehicles to Tumors Using Polyion Complexes and Gold Nanoparticles. *ACS Nano* **2014**, *8* (9), 8979–8991.

(8) Kataoka, K.; Harada, A.; Nagasaki, Y. Block Copolymer Micelles for Drug Delivery: Design, Characterization and Biological Significance. *Advanced Drug Delivery Reviews* **2012**, *64* (S), 37–48.

(9) López-Maldonado, E. A.; Oropeza-Guzmán, M. T.; Ochoa-Terán, A. Improving the Efficiency of a Coagulation-Flocculation Wastewater Treatment of the Semiconductor Industry Through Zeta Potential Measurements. *Journal of Chemistry* **2014**, *2014* (3), 1–10.

(10) Shi, L.; Carn, F.; Boué, F.; Mosser, G.; Buhler, E. Control Over the Electrostatic Self-Assembly of Nanoparticle Semiflexible Biopolyelectrolyte Complexes. *Soft Matter* **2013**, *9* (20), 5004–5012.

(11) Kaufman, G.; Nejati, S.; Sarfati, R.; Boltyanskiy, R.; Loewenberg, M.; Dufresne, E. R.; Osuji, C. O. Soft Microcapsules with Highly Plastic Shells Formed by Interfacial

Polyelectrolyte & Nanoparticle Complexation. *Soft Matter* **2015**, *11*, 7478–7482.

(12) Caruso, F.; Caruso, R. A.; Möhwald, H. Nanoengineering of Inorganic and Hybrid Hollow Spheres by Colloidal Templating. *Science* **1998**, 282 (6) 1111–1114.

(13) Wang, J.; Wang, J.; Ding, P.; Zhou, W.; Li, Y.; Drechsler, M.; Guo, X.; Cohen Stuart, M. A. A Supramolecular Crosslinker to Give Salt-Resistant Polyion Complex Micelles and Improved MRI Contrast Agents. *Angew. Chem.* **2018**, *130* (39), 12862–12866.

(14) Zhang, R.; Shklovskii, B. I. Phase Diagram of Solution of Oppositely Charged Polyelectrolytes. *Physica A: Statistical Mechanics and its Applications* **2005**, *352* (1), 216–238.

(15) Voets, I. K.; de Keizer, A.; Stuart, M. A. C. Advances in Colloid and Interface Science. *Advances in Colloid and Interface Science* **2009**, *147-148* (C), 300–318.

(16) Colby, R. H. Structure and Linear Viscoelasticity of Flexible Polymer Solutions: Comparison of Polyelectrolyte and Neutral Polymer Solutions. *Rheol Acta* **2009**, *49* (5), 425–442.

(17) Bungenberg de Jong, H.G., Kruyt, H.R. Coacervation. *Proceedings Royal Acad. Amsterdam* **1929,** 32, 849–856.

(18) Voorn, M.J., and Overbeek, J.T.G. Complex Coacervation. *Utrecht University* **1956** 1–80.

(19) Srivastava, S.; Tirrell, M. V. Polyelectrolyte Complexation. *Advances in Chemical Physics*, 2016, *161*, 499–544.

(20) Li, L.; Srivastava, S.; Andreev, M.; Marciel, A. B.; de Pablo, J. J.; Tirrell, M. V. Phase Behavior and Salt Partitioning in Polyelectrolyte Complex Coacervates. *Macromolecules* **2018**, *51* (8), 2988–2995.

(21) Cao, Q.; Bachmann, M. Electrostatic Complexation of Linear Polyelectrolytes with Soft Spherical Nanoparticles. *Chemical Physics Letters* **2013**, *586* (C), 51–55.

(22) Cao, Q.; Bachmann, M. Polyelectrolyte Adsorption on an Oppositely Charged Spherical Polyelectrolyte Brush. *Soft Matter* **2013**, *9* (20), 5087–12.

(23) Stoll, S.; Chodanowski, P. Polyelectrolyte Adsorption on an Oppositely Charged Spherical Particle. Chain Rigidity Effects. *Macromolecules* **2002**, *35* (25), 9556–9562.

(24) Pandav, G.; Ganesan, V. Computer Simulations of Dendrimer–Polyelectrolyte Complexes. *J. Phys. Chem. B* **2014**, *118* (34), 10297–10310.

(25) Pandav, G.; Pryamitsyn, V.; Errington, J.; Ganesan, V. Multibody Interactions, Phase Behavior, and Clustering in Nanoparticle–Polyelectrolyte Mixtures. *J. Phys. Chem. B* **2015**, *119* (45), 14536–14550.

(26) Ulrich, S.; Seijo, M.; Stoll, S. The Many Facets of Polyelectrolytes and Oppositely Charged Macroions Complex Formation. *Current Opinion in Colloid & Interface Science* **2006**, *11* (5), 268–272.

(27) Tong, C. The Numerical Study of the Adsorption of Flexible Polyelectrolytes with the Annealed Charge Distribution Onto an Oppositely Charged Sphere by the Self-Consistent Field Theory. *The Journal of Chemical Physics* **2013**, *139* (8), 084903–084910.

(28) Pryamitsyn, V.; Ganesan, V. Interplay Between Depletion and Electrostatic Interactions in Polyelectrolyte–Nanoparticle Systems. *Macromolecules* **2014**, *47* (17), 6095–6112.

(29) Obermeyer, A. C.; Mills, C. E.; Dong, X.-H.; Flores, R. J.; Olsen, B. D. Complex Coacervation of Supercharged Proteins with Polyelectrolytes. *Soft Matter* **2016**, *12*, 3570–3581.

(30) Messina, R.; Holm, C.; Kremer, K. Polyelectrolyte Adsorption and Multilayering on Charged Colloidal Particles. *J. Polym. Sci. B Polym. Phys.* **2004**, *42* (19), 3557–3570.

(31) Schiessel, H.; Rudnick, J.; Bruinsma, R.; Gelbart, W. M. Organized Condensation of Worm-Like Chains. *Europhys. Lett.* **2000**, *51* (2), 237–243.

(32) Kobayashi, M.; Juillerat, F.; Galletto, P.; Bowen, P.; Borkovec, M. Aggregation and Charging of Colloidal Silica Particles: Effect of Particle Size. *Langmuir* **2005**, *21*, 5761–5769.

(33) Wallin, T.; Linse, P. Monte Carlo Simulations of Polyelectrolytes at Charged Micelles. 1. Effects of Chain Flexibility. *Langmuir* **1996**, *12* (2), 305–314.

(34) Kumar, S.; Yadav, I.; Aswal, V. K.; Kohlbrecher, J. Structure and Interaction of Nanoparticle–Protein Complexes. *Langmuir* **2018**, *34* (20), 5679–5695.

(35) Jalil, A. H.; Pyell, U. Quantification of Zeta-Potential and Electrokinetic Surface Charge Density for Colloidal Silica Nanoparticles Dependent on Type and Concentration of the Counterion: Probing the Outer Helmholtz Plane. *J. Phys. Chem. C* **2018**, *122* (8), 4437–4453.